The SrLiAl$_3$N$_4$:Eu^{2+} Phosphor Synthesized by the Raw Material Model Obtained by DFT Calculations

Woon Bae Park[†]

Faculty of Nanotechnology and Advanced Materials Engineering, Sejong University, Seoul 05006, Korea

(Received March 20, 2017; Revised May 8, 2017; Accepted May 8, 2017)

ABSTRACT

Improvement studies of existing phosphors are needed for use in light emitting diodes (LEDs). Among the phosphors discovered recently, the SLA (SrLiAl$_3$N$_4$:Eu^{2+}) is a phosphor that has a narrow width. It is now known as a good red phosphor that meets the industry's needs for warm white (color temperature ranging from 2700 to 4000 K) and high CRI (> 80). However, SLA phosphors are obtained from difficult synthetic methods. All commercially available phosphors should be derived from the general solid state synthesis method. The phosphors produced by difficult synthetic methods will inevitably fall out of price competitiveness and will be scrapped. This study succeeded in synthesizing SLA (SrLiAl$_3$N$_4$:Eu^{2+}) phosphors by using a general solid phase synthesis method based on the reaction energy obtained from DFT calculations. As a result, we found an optimal solid state synthesis method for SLA phosphors.

Key words : Light emitting diode, Phosphor, DFT, Reaction energy, Solid state reaction

1. Introduction

As lighting technology continues to develop, energy efficiency has become a more critical standard for light devices. The international trend is that conventional fluorescent lamps or metal filament lamps, which consume too much energy, should be replaced by highly energy-efficient light emitting diode (LED) lamps to reduce energy consumption. This is because LED lamps are manufactured based on semiconductor technology that emit only monochromatic light. However, white light lamps should incorporate the entire spectrum of visual light. Hence, a phosphor-converted LED (pc-LED) can be produced by combining a yellowish green fluorescent substrate with a blue LED chip (440 to 480 nm) that emits blue light or by combining a green fluorescent substrate with a red fluorescent substrate to emit white light.

Most of the commercially available pc-LEDs employ only Ce^{3+}-doped Y$_3$Al$_5$O$_{12}$ (YAG). The YAG:Ce^{3+} fluorescent substrate absorbs blue light and emits a wide wavelength range of visual light from 500 to 700 nm. In addition, the YAG:Ce^{3+} fluorescent substrate has good chemical and thermal stability.[1,2] However, the YAG:Ce^{3+} fluorescent substrate emits little light in the red spectrum. Thus, the cool white light range (color temperature of 4000 to 8000 K) is limited, as it provides a limited color rendering index (CRI < 75). Current lamps require warm white light (color temperature of 2700 to 4000 K) and a high CRI (> 80).

Hence, the goals of the light industry are to make the pc-LED light emission be well adapted to visibility and to improve the color reproduction without lowering the energy efficiency, thus obtaining a high light-emitting efficiency from the pc-LEDs. The accomplishment of these goals is determined by the central wavelength and half-width of a red fluorescent substrate. At present, very few red fluorescent substrates satisfy the conditions of high energy conversion efficiency and good deterioration characteristics. Commercially available red fluorescent substrates are (Ca,Sr,Ba)$_2$Si$_5$N$_8$:Eu^{2+} and (Ca,Sr)AlSiN$_3$:Eu^{2+}.[3,4] These two red fluorescent substrates have a relatively wide light-emitting wavelength spectra, and some of the wavelengths are longer than 700 nm, which is the limit of human visibility. Therefore, these two red fluorescent substrates are unable to reach the maximum light-emitting efficiency of high quality warm-white pc-LED (CRI > 90). The sulfide-based fluorescent substrate, Sr$_{1-x}$Ca$_x$S:Eu^{2+}, is a narrow half-width fluorescent substrate that shows good light-emitting characteristics, but it is difficult to apply it to commercial products due to the decrease of the light-emitting efficiency depending on temperature, the high sensitivity to hydrolysis, and the toxicity of hydrolysis products (H$_2$S gas).[5]

Hence, a red narrow half-width fluorescent substrate that was recently discovered and reported by Schnick *et al.*, SLA (SrLiAl$_3$N$_4$:Eu^{2+}), has drawn much attention from the industry.[6] However, the experimental method reported by Schnick *et al.* includes a synthetic method that may not be easily applied to production. All the fluorescent substrates that are used commercially are generally obtained by a solid-state synthetic method. Therefore, a fluorescent substrate that can be produced by a difficult synthetic method

---

[†]Corresponding author : Woon Bae Park
 E-mail : imjinpp@sejong.ac.kr
 Tel : +82-2-3408-4477   Fax : +82-2-3408-4477

will have low price competitiveness and eventually be removed from the market.

In the present study, the SLA fluorescent substrate was synthesized by a general synthetic method and not by the difficult experimental method reported by Schnick *et al.* The experimental model was selected on the basis of the reaction energy obtained by performing density function theory (DFT) calculations, and not random experiments, to develop a general solid-state synthetic method.

2. Experimental Procedure

2.1. DFT Calculation

In the Vienna ab initio simulation package (VASP5.4),[7-10] the gradient approximation (GCA) method proposed by Perdew, Burke, and Ernzerhof (PBE),[11] as well as the Monkhorst-Pack method, was employed. The cut-off was set to be 500 eV, which is a general criterion, and the K-mesh appropriate for each structure was used.[12] In addition, the simulation was performed by adopting the Project Augmented Wave (PAW) pseudopotential,[13,14] which is generally used for each element. Structural relaxation was performed to enable the variation of the atomic positions, lattice parameters, and the values for symmetry. After completing the structural relaxation, the energy values were verified. The band structure as well as the density of state (DOS) were also examined to verify if the calculation was carried out normally.

2.2. Fabrication and Analysis

The raw material reagents selected through the DFT calculations (Sr, Li_3N, AlN, and EuN) were weighed and mixed according to the stoichiometry. They were then pulverized to prepare samples in a glove box that included oxygen and moisture less than 2 ppm. Then, 0.3 g of each sample was put into a boron nitride (BN) ($80 \times 40 \times 20$ mm) container that has 18 holes with a diameter of 8.5 mm. Subsequently, the BN container was transported to a sealed tube-type heat treatment system to calcinate the samples in a nitrogen atmosphere ($N_2:H_2$ = 95:5) at 1000°C for four hours. Each of the calcinated samples was then pulverized to undergo X-ray diffraction (XRD) and photoluminescence (PL) analysis. The emission spectrum was measured at 460 nm excitation by using a house-built continuous-wave (CW) PL system equipped with a xenon lamp.

3. Results and Discussion

3.1. Reaction energy calculation

The reactant energy and the product energy were obtained by the DFT calculation, and the reaction energy was calculated as the difference between the two energy values. The calculation results are shown in Table 1. Calculation was performed to obtain the energy values of the raw material reagents that were used as reactants in the SLA report,[6] which were SrH_2, $LiAlH_4$, AlN, and N, as well as the energy values of their products, which were $SrLiAl_3N_4$ and NH_3. The calculated reaction energy was –0.2224 eV/atom. The SLA fluorescent substrate[6] was synthesized by a general solid-state synthetic method, as described in the introduction. For this purpose, the selected raw materials were mostly nitrides. The selected raw materials were Sr, Li_3N, AlN, and N. In the case of Sr, the Sr metal was selected because the nitride reagent, Sr_3N_2, was not available. The calculated reaction energy was –0.1827 eV/atom. Comparison of the two reaction energy values showed that the method reported by the SLA report was more stable. However, the method chosen in the present study was found to be more stable when compared with the reaction energy values of similar inorganic compounds reported by Ceder,[15] thereby indicating that the synthetic method may be feasible.

In addition, since various raw material reagents were selected in the present study, the reaction energy of the individual reactants was calculated. A striking fact from the calculations was that a big difference in the calculation value was found only between the calculations performed by setting the source of Al as a metal and the calculations performed by setting the source of Al as AlN, regardless of the calculation methods. The calculated reaction energy value was about 5 to 6 times lower in the calculation performed by setting the Al source to be Al metal than in the calculation performed by setting the Al source to be AlN. This result was consistent with the optimal synthesis conditions for a series of nitride fluorescent substrates that are commercially applied. For example, the CASN ($CaAlSiN_3:Eu^{2+}$) nitride red fluorescent substrate is synthesized by using the AlSi alloy metal as a raw material. Another example is the LSN ($La_3Si_6N_{11}:Ce^{3+}$) yellow fluorescent substrate that is synthesized by using the $LaSi_2$ alloy metal as a raw material. These examples show that the possibility of synthesis increases when the Al metal is used as the Al source.
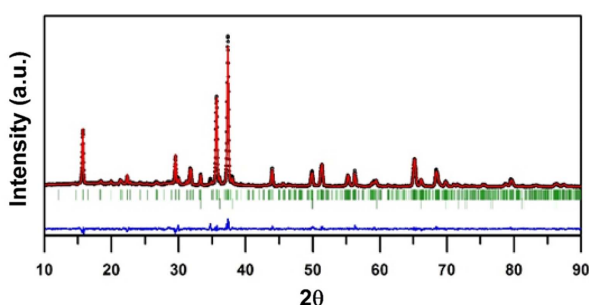
Table 1. Computed Reaction Energies

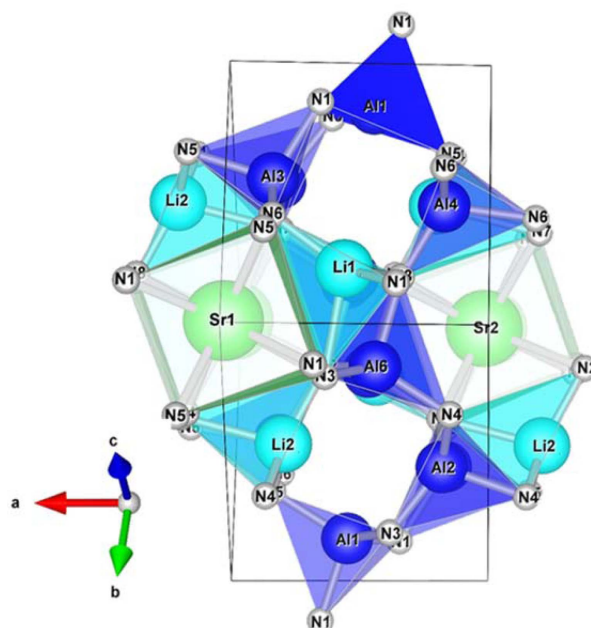|	Reaction	Reaction Energy (eV/atom)
1	$SrH_2+LiAlH_4+2AlN+4N \rightarrow SrLiAl_3N_4+2NH_3\uparrow$	–0.2224
2	$Sr+1/3Li_3N+3AlN+2/3N \rightarrow SrLiAl_3N_4$	–0.1827
3	$Sr+Li+3AlN+N \rightarrow SrLiAl_3N_4$	–0.2611
4	$Sr+Li+3Al+4N \rightarrow SrLiAl_3N_4$	–1.2925
5	$Sr+1/3Li_3N+3Al+11/3N \rightarrow SrLiAl_3N_4$	–1.2142

However, the correlation between the reaction energy and the synthetic route roughly explained in the present article does not provide an absolute standard of value. In particular, the DFT calculations performed in the present study are based on the simple thermodynamic internal energy at the absolute temperature of zero (0) under the assumption that all materials are solid. Therefore, the values obtained from the calculations do not represent the actual situation at high temperature involving many gas phases. It should be noted that the entropy term representing the gas phases was completely neglected and the kinetic term may not be considered in the simple DFT calculations. Nevertheless, considering that the reaction energy values obtained from the simplified calculations of the present study are well matched with the situation of the actual experiment, the calculation results may be used to predict the optimal conditions for synthesizing fluorescent substrates.

3.2. Structural properties

Based on the calculation results, the synthesis was performed by the Method No. 2 shown in Table 1. An XRD analysis was performed to verify if the synthesis of the SLA fluorescent substrate was well carried out. The calcinated samples did not have a single phase SLA structure, but included a small amount of impurity. The impurity phase was AlN, which was consistent with the reaction energy calculation results that showed the reaction energy value increasing when the AlN source was used. Fig. 1 shows the XRD pattern and the Rietveld refinement results of the SLA fluorescent substrate. The sample had a triclinic system structure in the P-1 space group. The lattice parameters were a = 5.8461 (2) Å, b = 7.4791 (4) Å, c = 9.9199 (4) Å, α = 83.598 (2)°, β = 76.766 (5)°, and γ = 79.519 (6)°. In addition, the lattice parameters of the impurity phase, AlN, were a = 3.1082 (1) Å, and c = 4.9743 (5) Å. The space group was also found to be P6₃mc. Besides the AlN impurity phase, some unidentified peaks that were extremely small and weak

Fig. 2. Crystal structure of SLA (SrLiAl₃N₄:Eu²⁺) viewed along [011] directions.

were also found. The atomic position table reported by the SLA report from Schnick et al.[6] was selected as the initial Rietveld model. The Rietveld refinement was performed by using the Fullprof package. In the process of the Rietveld refinement, such variables as scale factor, zero correction, background, half-width, lattice, atom position, and thermal were optimized through the refinement procedures. The blue line in Fig. 1, which represents the difference between the experimental value and the calculated value, is almost flat. Hence, the profile consistency coefficients were as good as Rp = 6.44, Rwp = 8.43, and Rexp = 7.89 with x^2 = 1.14, indicating that the calculated profile was well matched with the experimental values. Despite the presence of unidentified peaks of impurities that could not be considered in the Rietveld refinement procedures, the value of x^2 was unaffected. Fig. 2 shows the shape of the structure viewed from the [011] direction, as calculated by the VESTA software. The overall structure is that of a host lattice having a high-density and rigid framework with aligned edges of AlN₄ and LiN₄ tetrahedron (AlN: 1.87 to 2.00 Å and LiN: 1.98 to 2.10 Å). A vierer ring channel was obtained along the [011] direction. The negative charge of the [LiAl₃N₄]²⁻ framework net structure was offset by integrating the Sr²⁺ ion. The SLA fluorescent structure that has a highly symmetric hexahedron (8 N atoms Sr-N: 2.69 ~ 2.91 Å) is very advantageous for narrow half-width light emitting as it has two different crystallographic Sr sites. The SrN₈ polyhedron is infinitely generated along the [011] direction as it is connected with a common plane, and the Sr-Sr distance is 3.27 Å. In the eight coordinates, the ionic radius of Eu²⁺ was 1.25 Å, which was almost equal to that of Sr²⁺ (1.26 Å). Therefore, the Sr²⁺ site may be occupied by the Eu²⁺ ion.
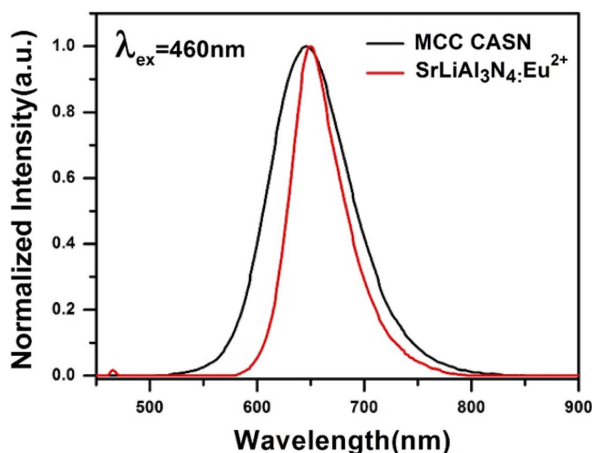

Fig. 1. Observed (dots), calculated (red line), and difference (blue line) profiles obtained after full pattern Rietveld refinement of SLA (SrLiAl₃N₄:Eu²⁺) using a Triclinic structure in the P-1 space group in the 2θ and in the range of 10 to 90°. The vertical tick marks above the difference profiles in the first and second lines, respectively, from the top denote the position of Bragg reflections for the SLA (SrLiAl₃N₄:Eu²⁺) phase and impurity phases AlN (P6₃mc space group).

Fig. 3. Emission spectra for SLA (SrLiAl$_3$N$_4$:Eu^{2+}) and CASN (CaAlSiN$_3$:Eu^{2+}).

3.3. Luminescence of SLA (SrLiAl$_3$N$_4$:Eu^{2+})

Figure 3 shows the emission spectrum of the synthesized SLA fluorescent substrate and that of the CASN fluorescent substrate that is commercially used. The half-width is narrower in the emission spectrum of the synthesized SLA fluorescent substrate than in that of the CASN fluorescent substrate, which is consistent with the report by Schnick *et al.*.[6] The red fluorescent substrate that has such a narrow half-width has advantages in the preparation of high-quality warm-white pc-LED (CRI > 90). According to the experimental design obtained from the reaction energy calculations, the synthesis resulted in a good SLA fluorescent substrate structure, as shown by the emission spectrum, despite the presence of the AlN impurity. The larger Stokes shift and the broader emission spectrum band observed in the Eu^{2+} fluorescent substrate has been generally correlated with the asymmetric dopant site geometry.[16] The 4f^{6}5d^1 energy level of Eu^{2+} and the transition in the 4f^7(^{8}S$_{7/2}$) → 4f^6(^{7}F)5d^1 inorganic host are transformed by the covalent bond and the polarization possibility of the Eu^{2+}-ligand interaction.[17-20] The activator ions in the SLA are surrounded by a network of condensed AlN$_4$ and LiN$_4$ tetrahedrons. Therefore, the more polarizable circumstance of nitrides provides a stronger nephelauxetic effect than that of, for example, an oxide environment, which results in a greater crystal field splitting and a stronger ionic character to lower the 4f^{6}5d^1 excitation state of Eu^{2+}. Since the energy difference between the 4f^7 ground state and the 4f^{6}5d^1 excited state is reduced, the absorption and the light-emitting transition shift to the red spectrum region.

4. Conclusions

The present study was conducted to replace the difficult SLA fluorescent substrate synthetic method reported by Schnick *et al.* This is because all the fluorescent substrates that are commercially used are manufactured by general solid-state synthetic methods. However, the synthetic method reported by Schnick *et al.* has little commercial feasibility, unavoidably resulting in a high price. No matter how good a fluorescent substrate may be, an alternative material is pursued if the price competitiveness is low in the industrial field. In the present study, general raw materials were selected on the basis of the reaction energy values obtained through DFT calculations, and the synthesis was carried out by a general solid-state synthetic method. The structure of the synthesized fluorescent substrate was verified through Rietveld refinement. The emission spectrum showed that the experiment was carried out well. The presence of AlN impurity may be addressed by further optimization procedures.

Acknowledgments

REFERENCES

1. A. A. Setlur, "Phosphors for LED-based Solid-State Lighting," *Electrochem. Soc. Interface,* **16** [4] 32-6 (2009).
2. D. J. Robbins, "The Effects of Crystal Field and Temperature on the Photoluminescence Excitation Efficiency of Ce^{3+} in YAG," *J. Electrochem. Soc.,* **126** [9] 1150-55 (1979).
3. K. Uheda, N. Hirosaki, and H. Yamamoto, "Host Lattice Materials in the System Ca$_3$N$_2$-AlN-Si$_3$N$_4$ for White Light Emitting Diode," *Phys. Status Solidi A,* **203** [11] 2712-17 (2006).
4. K. Uheda, N. Hirodaki, Y. Yamamoto, A. Naito, T. Nakajima, and H. Yamamoto, "Luminescence Properties of a Red Phosphor, CaAlSiN$_3$:Eu^{2+}, for White Light-Emitting Diodes," *Electrochem. Solid-State Lett.,* **9** [4] H22-5 (2006).
5. R. Mueller-Mach and G. Mueller, "White Light Emitting Diodes for Illumination," *Proc. SPIE,* **3938** 30-41 (2000).
6. P. Pust, V. Weiler, C. Hecht, A. Tücks, A. S. Wochnik, A.-K. Henß, D. Wiechert, C. Scheu, P. J. Schmidt, and W. Schnick, "Narrow-Band Red-Emitting Sr[LiAl$_3$N$_4$]:Eu^{2+} as a Next-Generation LED-Phosphor material," *Nat. Mater.*, **13** [9] 891-96 (2014).
7. G. Kresse and J. Hafner, "Ab initio Molecular Dynamics for Liquid Metals," *Phys. Rev. B,* **47** [1] 558-61 (1993).
8. G. Kresse and J. Hafner, "Ab initio Molecular-Dynamics Simulation of the Liquid-Metal-Amorphous-Semiconductor Transition in Germanium," *Phys. Rev. B,* **49** [20] 14251-69 (1994).
9. G. Kresse and J. Furthmüller, "Efficiency of Ab-initio Total Energy Calculations for Metals and Semiconductors Using a Plane-Wave Basis Set," *Comput. Mater. Sci.,* **6** [1] 15-50 (1996).
10. G. Kresse and J. Furthmüller, "Efficient Iterative Schemes for Ab Initio Total-Energy Calculations Using a Plane-Wave Basis Set," *Phys. Rev. B,* **54** [16] 11169-86 (1996).
11. J. P. Perdew, K. Burke, and M. Ernzerhof, "Generalized Gradient Approximation Made Simple," *Phys. Rev. Lett.,* **77**

[18] 3865-68 (1996).

12. H. J. Monkhorst and J. D. Pack, "Special Points for Brillouin-Zone Integrations," *Phys. Rev. B.,* **13** [12] 5188-92 (1976).

13. P. E. Blöchl, "Projector Augmented-Wave Method," *Phys. Rev. B,* **50** [24] 17953-79 (1994).

14. G. Kresse and D. Joubert, "From Ultrasoft Pseudopotentials to the Projector Augmented-Wave Method," *Phys. Rev. B,* **59** [3] 1758-75 (1999).

15. G. Hautier, S. P. Ong, A. Jain, C. J. Moore, and G. Ceder, "Accuracy of Density Functional Theory in Predicting Formation Energies of Ternary Oxides from Binary Oxides and its Implication on Phase Stability," *Phys. Rev. B,* **85** [15] 155208 (2012).

16. G. J. Dirksen and G. Blasse, "Luminescence in the Pentaborate LiBa$_2$B$_5$O$_{10}$," *J. Solid State Chem.,* **92** [2] 591-93 (1991).

17. P. Dorenbos, "A Review on How Lanthanide Impurity Levels Change with Chemistry and Structure of Inorganic Compounds," *ECS J. Solid State Sci. Technol.,* **2** [2] R3001-11 (2013).

18. P. Dorenbos, "5d-Level Energies of Ce^{3+} and the Crystalline Environment. I. Fluoride Compounds," *Phys. Rev. B,* **62** [23] 15640-49 (2000).

19. P. Dorenbos, "5d-level Energies of Ce^{3+} and the Crystalline Environment. III. Oxides Containing Ionic Complexes," *Phys. Rev. B,* **64** [12] 125117 (2001).

20. P. Dorenbos, "Relating the Energy of the [Xe]5d^1 Configuration of Ce^{3+} in Inorganic Compounds with Anion Polarizability and Cation Electronegativity," *Phys. Rev. B,* **65** [23] 235110 (2002).